

2016

# A Comprehensive Evaluation of Regression Uncertainty and the Effect of Sample Size on the AHRI-540 Method of Compressor Performance Representation

Vikrant Aute

*Center for Environmental Energy Engineering, University of Maryland, College Park, vikrant@umd.edu*

Cara Martin

*Optimized Thermal Systems, Inc., Beltsville, MD, USA, cmartin@optimizedthermalsystems.com*

Follow this and additional works at: <http://docs.lib.purdue.edu/icec>

---

Aute, Vikrant and Martin, Cara, "A Comprehensive Evaluation of Regression Uncertainty and the Effect of Sample Size on the AHRI-540 Method of Compressor Performance Representation" (2016). *International Compressor Engineering Conference*. Paper 2457. <http://docs.lib.purdue.edu/icec/2457>

This document has been made available through Purdue e-Pubs, a service of the Purdue University Libraries. Please contact [epubs@purdue.edu](mailto:epubs@purdue.edu) for additional information.

Complete proceedings may be acquired in print and on CD-ROM directly from the Ray W. Herrick Laboratories at <https://engineering.purdue.edu/Herrick/Events/orderlit.html>

# A Comprehensive Evaluation of Regression Uncertainty and the Effect of Sample Size on the AHRI-540 Method of Compressor Performance Representation

Vikrant AUTE<sup>1\*</sup>, Cara MARTIN<sup>2</sup>

<sup>1</sup>University of Maryland College Park, Center for Environmental Energy Engineering,  
College Park, MD, USA  
(301-405-8726, [vikrant@umd.edu](mailto:vikrant@umd.edu))

<sup>2</sup>Optimized Thermal Systems, Inc.  
Beltsville, MD, USA  
(866-485-8233 x27, [cmartin@optimizedthermalsystems.com](mailto:cmartin@optimizedthermalsystems.com))

\* Corresponding Author

## ABSTRACT

AHRI Standard 540 (AHRI, 2015) is the current standard defining the methods for representing compressor performance data. The standard is widely used across the industry and uses a 10-coefficient third order polynomial equation to represent compressor published ratings. The accuracy of the data representation can be affected by multiple factors including measurement uncertainty, regression uncertainty, compressor to compressor variation, and operation outside of the normal operating envelope (extrapolation). In addition, the number and location of points in the operating envelope also affects the accuracy of the resulting 10-coefficient polynomial. The measurement uncertainty is well known and can be factored into the data reduction. However, the measurement uncertainty is generally not propagated into the regression uncertainty and hence the overall uncertainty in prediction using the polynomial is not known. This uncertainty also changes according to the number of samples used for developing the polynomial.

As a first step of the evaluation, a regression uncertainty analysis was conducted using a Monte Carlo simulation method. Results showed that the average uncertainty in mass flow rate prediction can be as high as 4% and that in power prediction can be as high as 5%. Error in predicted power and mass flow rate is higher for larger capacity compressors. For most compressors, the high errors occur in the region of the envelope with low suction and low discharge dew point temperatures.

A study of sampling considering different sample sizes and multiple sampling methods was conducted. Two additional methods of compressor performance representation were also analyzed. This analysis was presented with several challenges, particularly since the compressor operating envelope is a non-rectangular domain. A sampling method using Latin Hypercube Sampling (LHS) design and a proposed alternative sampling method based on polygonal design of experiments (PDOE) were evaluated. The resulting models were validated against a measured data set of more than 600 points encompassing the operating envelope for each compressor. In general, both the LHS and PDOE methods yielded similar errors in mass flow rate for sample sizes of 12, 14 and 16. Thus, for mass flow rate, it is possible to build a model with 12 systematically selected test points. For power prediction, the average error for the LHS and PDOE methods using AHRI Standard 540 and two other methods was lower than 2% for all sample sizes.

## 1. INTRODUCTION

The current performance rating standard for positive displacement compressors requires manufacturers to report tabular performance data over a specified operating envelope. The data is usually generated using a 10-coefficient third order polynomial equation. The coefficients for the equation are derived from measured and/or extrapolated

values using the method of “Least Squares”. This equation is also frequently used by manufacturers to represent the tabular data in a form suitable for use in simulation programs.

The original intent of this reporting method was to provide a consistent and uniform way of presenting performance data to enable manufacturers to evaluate different compressors for a particular application. Manufacturers also desire to use compressor performance with simulation tools to calculate system performance values for rating purposes. The current equation that is used to represent the data does not, however, always provide sufficient accuracy to meet the need for product rating. Furthermore, due to the costs involved with collecting the measured data, there is a desire to use the fewest number of data points. No specific information is provided to understand the impact of the number and distribution of measured test points to achieve a particular level of accuracy. Other sources of uncertainty are associated with the variation of measurement reproducibility across the application envelope as well as the compressor to compressor variation. An improvement in the method for representing data will likely enable an improvement in the accuracy of the product ratings without increasing the cost of generating the data.

## 2. DATA USED FOR ANALYSIS

A total of 29 sets of raw compressor data were used to evaluate the current method of developing a representative compressor performance map from experimental data. As can be seen from Table 1, data accounted for three types of compressors (reciprocating, rotary and scroll) over a complete capacity range for both pure fluids (R134a and R22) and mixed refrigerants (R404A and R410A). Data for multiple compressors of the same model were also acquired to evaluate the impact of unit to unit variation. Data generally included compressor geometry, operating conditions (pressure, temperature, mass flow rate, superheat, etc.), performance, instrument uncertainties, and Standard 540 coefficients.

**Table 1:** Data Set Used for Project Analysis

| Compressor Type                    | Application | Refrigerant | Capacity Range                                | Number of Data Sets | Number of Units Per Model |
|------------------------------------|-------------|-------------|---|---------------------|---------------------------|
| Reciprocating                      | A/C & HP    | R410A       | 670 – 19,079 W<br>(2,285 – 65,099 Btu/hr)     | 9                   | 2-3                       |
|                                    |             | R22         | 1,487 – 10,574 W<br>(5,075 – 36,079 Btu/hr)   | 2                   | 3                         |
|                                    | Low Temp.   | R404A       | 532 – 3,028 W<br>(1,816 – 10,331 Btu/hr)      | 1                   | 1                         |
|                                    |             |             | 751 – 3,951 W<br>(2,564 – 13,483 Btu/hr)      | 1                   | 1                         |
|                                    | High Temp.  | R407C       | 1,644 – 11,988 W<br>(5,611 – 40,906 Btu/hr)   | 1                   | 1                         |
|                                    |             | R134a       | 858 – 3,733 W<br>(2,929 – 12,739 Btu/hr)      | 1                   | 1                         |
| Scroll                             | A/C & HP    | R410A       | 1,762 – 227,460 W<br>(6,013 – 776,125 Btu/hr) | 8                   | 1                         |
|                                    | Low Temp.   | R404A       | 1,420 – 5,853 W<br>(4,844 – 19,970 Btu/hr)    | 1                   | 1                         |
| Rotary                             | A/C & HP    | R410A       | 1,125 – 13,020 W<br>(3,838 – 44,427 Btu/hr)   | 2                   | 1                         |
|                                    |             | R134a       | 446 – 5,479 W<br>(1,523 – 18,695 Btu/hr)      | 2                   | 1                         |
|                                    |             | R407C       | 1,411 – 6,111 W<br>(4,813 – 20,851 Btu/hr)    | 1                   | 1                         |
| Total Complete Data Sets Available |             |             |   | 29                  |                           |

### 3. REGRESSION UNCERTAINTY ANALYSIS

Experimental measurements involve uncertainty due to various sources and it is important to characterize the effect of measurement uncertainties on the regression coefficients (Coleman and Steele, 2009). This helps us to better understand the effect of measurement uncertainty on the values predicted by the compressor map and the corresponding uncertainty when the map is used for system rating. The uncertainty information can then be used in understanding the effect of tolerances used in the various rating and enforcement tests. The typical data used in the map are measured temperatures, mass flow rate and power consumption. These are all measured quantities (and not derived) and hence no uncertainty propagation is required. A Monte Carlo simulation method was used to conduct a regression uncertainty analysis for the provided compressor map data.

#### 3.1 Approach

In the case of compressor testing, the measured quantities include the suction and discharge dew point temperatures, the power consumption and the mass flow rate. The ASHRAE Standard 23 provides the required measurement accuracies for these quantities, which are depicted in Table 2.

*Table 2: Measurement accuracies*

| Quantity       | Accuracy                 |
|----------------|--------------------------|
| Temperature    | 0.5°F                    |
| Power          | 1% of measured value     |
| Mass flow rate | 1% of the measured value |

Random errors also occur during the course of actual experiments. These errors are included in the measurements, but are not quantitatively identified. For the purposes of the Monte Carlo analysis, the various measurement errors were assumed to be normally distributed with a mean value as the measured value reported in the data sets and the standard deviation as the accuracy value reported in Table 2. This practice is not normally advised since the actual standard deviation will be lower, but it was used here to account for the overall measurement uncertainties including both systematic and random errors.

The following steps describe the Monte Carlo simulation carried out for each of the 29 data sets shown in Table 1. Assume that there are 50 data points in a single data set.

1. Generate 25,000 data sets, based on normal distribution, each comprising of 50 data points. 25,000 sets was found to be a reasonably good number to minimize computational time while maintaining a good level of accuracy.
2. Develop a regression model (curve fit) for each data set, based on the 10-coefficient polynomial. One model each is developed for power consumption and mass flow rate, as a function of  $T_e$  and  $T_c$ .
3. Predict each point in the original dataset using the regression models. Thus, for each of the 50 points, there are 25,000 predicted values for power consumption.
4. Compute the mean and the standard deviation of the 25,000 predicted values. The difference between this mean value and the measured value is termed as the Error in Mean. The ratio of the standard deviation and the mean is termed as the coefficient of variance (COV) and is expressed as a percentage of the mean.
5. For each of the 25,000 predicted values, compute the individual errors, i.e., the difference between predicted power consumption at that point (i.e.,  $[T_e, T_c]$ ) and the measured value. The maximum absolute percent error (MAPE), which indicates the worst case prediction error in mass flow rate (or power) over the entire operating envelop, can then be computed for each of these 50 points.
6. The error in mean and the maximum absolute error can then be plotted on  $[T_e, T_c]$  plot representing the compressor operating envelope. Thus for each compressor dataset, we can generate four plots (i.e., two each for mass flow rate and power consumption).

#### 3.2 Results

A sample of the plots generated for each data set is shown in Figure 1. Results are summarized in Table 3. Based on the error metrics and the individual analysis of each of the plots generated for all data sets, the following general conclusions can be drawn:

1. The minimum absolute error in the predicted mean power is 0.2% and the maximum error in the predicted mean power is 5%. The maximum COV is 1.7%.

2. The minimum absolute error in predicted mean mass flow rate is 0.4% and the maximum error in the predicted mean mass flow rate is 4.3%. The maximum COV is 3.5%.
3. The worst case maximum absolute error in predicted power is 9%.
4. The worst case maximum absolute error in predicted mass flow rate is 17%.
5. In general, the maximum (worst case) errors in mass flow rate prediction are much higher than those in power prediction.
6. For most compressors, the highest errors occur in Quadrant-3, i.e., low suction dew point and low discharge dew point region. These are the compressors that have “sufficient” number of data points distributed across the entire operating envelope.
7. Refrigerants R134a, R404A and R407C exhibit higher errors compared to R410A, but the corresponding datasets do not have ‘sufficient’ points to begin with. As such these errors could be due to insufficient data available for regression.
8. Larger compressors (i.e., high power and mass flow rate values) exhibit higher errors.

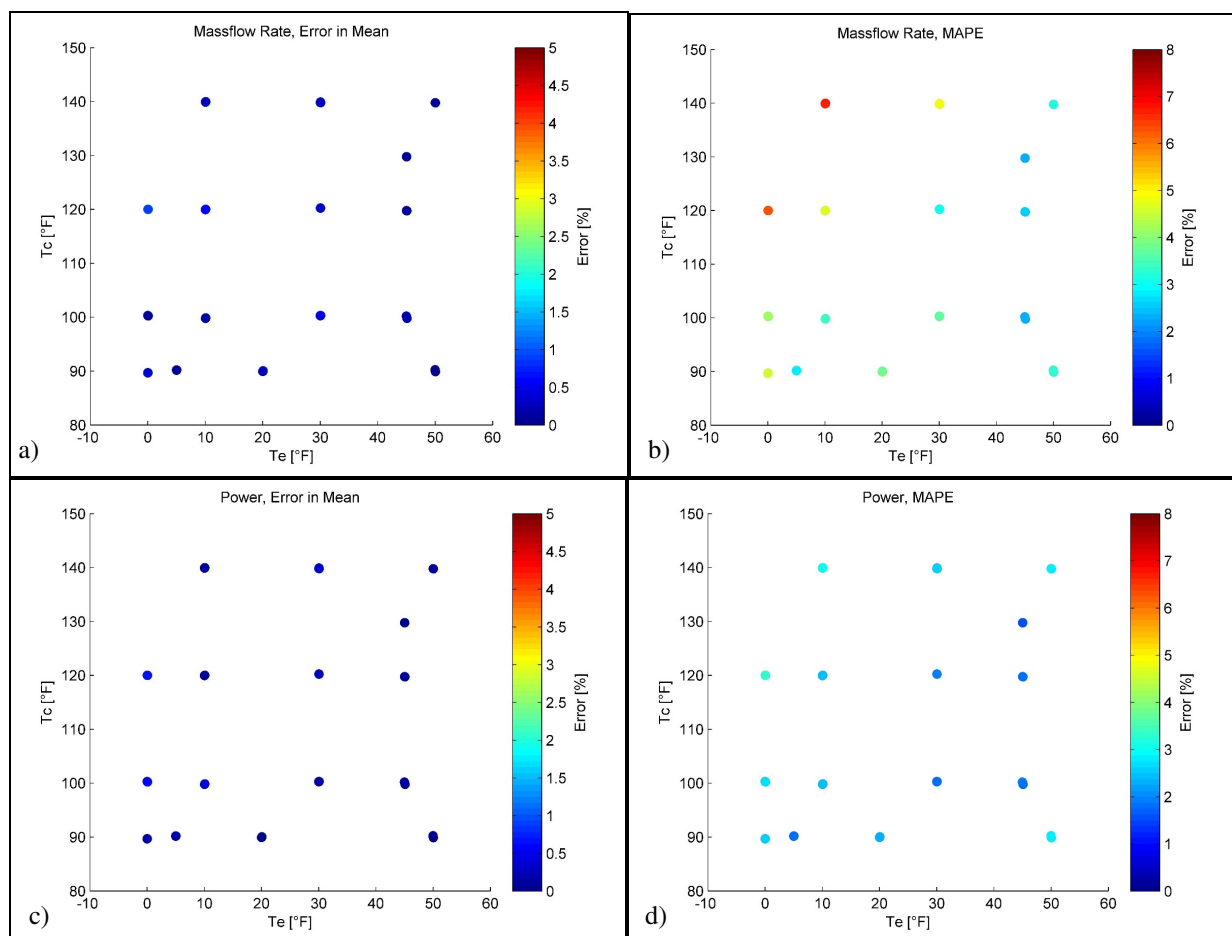


**Figure 1:** Monte Carlo simulation results for R22 compressor showing (a) error in mean mass flow rate, (b) maximum absolute percent error in mass flow rate, (c) error in mean power, and (d) maximum absolute percent error in predicted power

Table 3: Monte Carlo simulation results

| Fluid | Test Points | Power Max. Error in Mean [%] | Power COV [%] | Power MAPE [%] | Mass Flow Max. Error in Mean [%] | Mass flow COV [%] | Mass flow MAPE [%] |
|-------|-------------|------------------------------|---------------|----------------|----------------------------------|-------------------|--------------------|
| R134a | 17          | 1.09                         | 1.18          | 5.82           | 1.12                             | 1.82              | 9.03               |
| R134a | 17          | 0.56                         | 1.25          | 6.00           | 0.80                             | 2.10              | 12.49              |
| R134a | 17          | 1.87                         | 1.29          | 6.16           | 0.68                             | 2.00              | 9.21               |
| R22   | 48          | 0.63                         | 0.77          | 3.31           | 0.96                             | 1.39              | 6.87               |
| R22   | 48          | 0.98                         | 0.79          | 3.78           | 2.81                             | 1.50              | 7.54               |
| R22   | 49          | 0.64                         | 0.76          | 3.73           | 1.40                             | 1.44              | 7.15               |
| R22   | 48          | 0.38                         | 0.76          | 3.06           | 0.67                             | 1.39              | 6.22               |
| R22   | 49          | 0.56                         | 0.75          | 3.57           | 0.75                             | 1.28              | 6.22               |
| R22   | 49          | 0.45                         | 0.74          | 3.74           | 4.33                             | 1.19              | 9.03               |
| R404A | 17          | 2.04                         | 1.53          | 8.60           | 3.16                             | 2.55              | 16.08              |
| R404A | 22          | 3.38                         | 1.21          | 7.66           | 2.23                             | 1.94              | 8.98               |
| R404A | 21          | 2.27                         | 1.31          | 7.62           | 1.70                             | 2.50              | 13.02              |
| R407C | 19          | 0.76                         | 1.22          | 5.86           | 4.36                             | 2.28              | 15.31              |
| R407C | 18          | 2.81                         | 1.46          | 7.31           | 4.19                             | 2.36              | 14.02              |
| R410A | 21          | 5.09                         | 1.27          | 7.07           | 1.13                             | 1.90              | 7.77               |
| R410A | 16          | 0.21                         | 1.09          | 5.03           | 1.89                             | 1.92              | 10.27              |
| R410A | 16          | 0.88                         | 1.73          | 9.10           | 1.88                             | 3.51              | 17.40              |
| R410A | 17          | 0.75                         | 1.31          | 5.86           | 0.98                             | 2.62              | 12.65              |
| R410A | 17          | 2.52                         | 1.47          | 7.25           | 1.67                             | 2.98              | 13.01              |
| R410A | 21          | 1.44                         | 1.32          | 5.63           | 2.79                             | 2.05              | 13.51              |
| R410A | 19          | 0.41                         | 1.13          | 4.94           | 0.41                             | 1.54              | 6.72               |
| R410A | 20          | 12.28                        | 1.12          | 15.37          | 3.06                             | 1.48              | 7.01               |
| R410A | 22          | 0.34                         | 1.15          | 6.06           | 0.99                             | 1.71              | 8.23               |
| R410A | 21          | 1.19                         | 1.16          | 6.60           | 0.59                             | 1.57              | 7.58               |
| R410A | 23          | 0.90                         | 1.21          | 5.99           | 0.47                             | 1.64              | 8.68               |
| R410A | 21          | 1.34                         | 1.15          | 5.50           | 0.73                             | 1.58              | 7.70               |
| R410A | 49          | 1.17                         | 1.28          | 6.16           | 1.47                             | 2.90              | 12.96              |
| R410A | 50          | 0.79                         | 1.03          | 5.10           | 1.61                             | 2.22              | 11.16              |
| R410A | 49          | 1.40                         | 1.05          | 5.12           | 2.20                             | 2.46              | 11.33              |
| R410A | 49          | 0.71                         | 0.80          | 3.54           | 0.79                             | 1.17              | 5.55               |
| R410A | 49          | 0.52                         | 0.78          | 3.44           | 0.72                             | 1.22              | 5.45               |
| R410A | 50          | 0.62                         | 0.76          | 3.95           | 1.78                             | 1.26              | 6.97               |
| R410A | 49          | 0.86                         | 1.04          | 5.02           | 1.96                             | 2.57              | 11.97              |
| R410A | 47          | 1.09                         | 1.14          | 4.55           | 2.28                             | 2.51              | 12.01              |
| R410A | 48          | 0.36                         | 0.87          | 3.83           | 1.70                             | 1.98              | 9.13               |
| R410A | 52          | 0.63                         | 0.77          | 3.58           | 2.15                             | 1.66              | 7.89               |
| R410A | 52          | 0.48                         | 0.84          | 3.89           | 3.53                             | 1.78              | 9.38               |
| R410A | 52          | 0.54                         | 0.88          | 4.05           | 3.09                             | 1.84              | 8.46               |
| R410A | 49          | 0.37                         | 0.79          | 3.38           | 0.65                             | 1.25              | 5.88               |
| R410A | 49          | 0.36                         | 0.80          | 3.78           | 1.00                             | 1.25              | 6.23               |
| R410A | 49          | 1.14                         | 0.79          | 3.36           | 1.07                             | 1.22              | 6.66               |
| R410A | 48          | 0.70                         | 0.80          | 3.59           | 0.47                             | 1.22              | 5.76               |
| R410A | 48          | 0.76                         | 0.79          | 3.83           | 0.59                             | 1.19              | 5.33               |
| R410A | 48          | 0.91                         | 0.81          | 3.96           | 0.96                             | 1.26              | 5.87               |

## 4. SAMPLING STUDY

A study was conducted to evaluate and understand the influence of different sampling methods. Based on feedback received from manufacturing partners, there is no well-established methodology used in selecting the sample points for developing the 10-coefficient map. Two approaches were considered, a conventional approach using a Latin Hypercube Sampling (LHS) design, and a Polygon Design of Experiments (PDOE) method taking into account non-rectangular domains.

### 4.1 Conventional Sampling Using the Latin Hypercube Sampling (LHS) Design

A sampling study using the LHS method was conducted. The map data set contains a total of 16 points such that 15 points are selected for use in the analysis. The sampling study consisted of the following steps:

1. Use the provided map data to develop a 10-coefficient polynomial model for mass flow rate and power consumption. Verify these models against the comprehensive data set.
2. Using the comprehensive verification dataset, develop a regression surface using the Kriging metamodel. The Kriging metamodel does not require a functional form and is capable of exactly reproducing the source data.
3. Select 15 points from the operating envelope.
4. Compute the mass flow rate and power consumption using the Kriging metamodel for the sampled points.
5. Develop a 10-coefficient polynomial model based on the data from Step-4.
6. Verify the model from Step-5 against the comprehensive data set.

Figure 2 shows sample plots generated for the errors in predicted mass flow rate for a given compressor data set. Similar plots resulted for predicted power. Based on these and other results, the 10-coefficient polynomial obtained using the LHS samples is more accurate (lower errors) in terms of both mass flow rate and the power consumption over the entire operating envelope, including some extrapolation. Based on this preliminary analysis, the LHS sampling may be better suited for use with the 10-coefficient map. The challenge with LHS sampling, however, is that it is based on a random number generator. As such, the samples can change from run to run and the accuracy may not be reproducible. Furthermore, conventional sampling techniques are designed to work with square or rectangular domains. Due to availability of over 600 data points encompassing the entire operating envelope, it was possible to use the LHS method for sampling for use with the AHRI-540 model in this particular analysis. Ultimately, for the analysis conducted, the LHS method yielded average errors lower than 2% for all sample sizes.

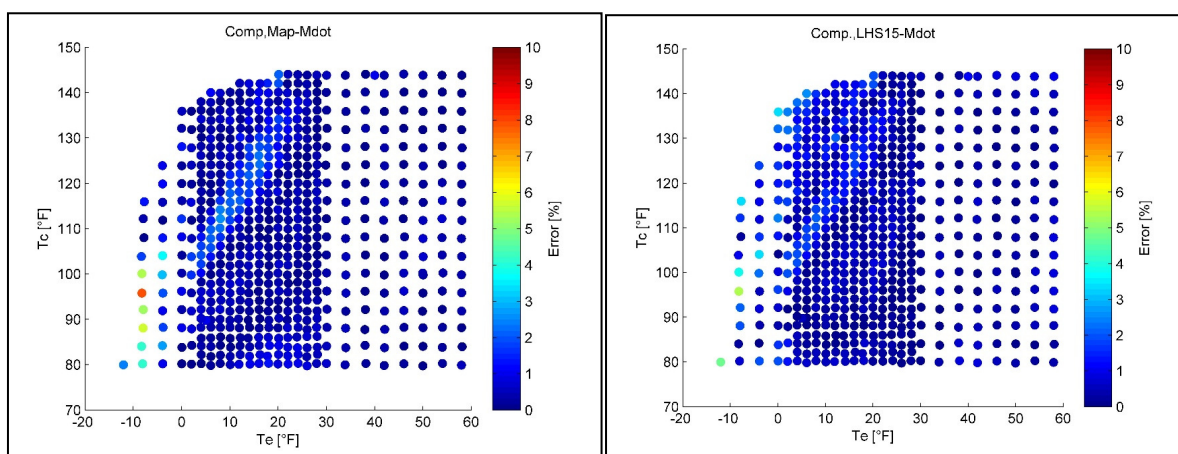


**Figure 2:** Comparison of errors in predicted mass flow rate for map data vs. LHS samples

### 4.2 Non-Rectangular Domains

The compressor operating envelope is non-rectangular, and hence, conventional sampling techniques are not directly applicable for selecting test points. A mathematically sound approach is required to handle non-rectangular domains. The two main methods published on space-filling designs for non-rectangular domains are Draguljic et al. (2012) and Lekivetz and Jones (2014). There is no open-source implementation available for either of the two methods, and

hence, the method by Lekivetz and Jones (2014) was implemented with some simplifications for use in the conducted analysis. Consider a non-rectangular 2-D domain such as a compressor operating envelope represented on a [Te,Tc] plot. Assume it is desired to sample  $n$  points inside this domain. The steps in the approach are as follows:

1. Start with the non-rectangular domain.
2. Generate a large number of candidate sample points, either randomly or based on a uniform grid. These candidate sample points are superimposed on the design domain. Using the conventional methods, such points are generated on a rectangular domain, hence these points will span beyond the operating envelope (or domain).
3. Filter the candidate sample points that are outside the operating domain.
4. Use a clustering algorithm to generate  $n$  clusters based on a Euclidean distance metric.
5. Compute the convex hull for each of these clusters. Note that some of the polygons corresponding to the convex hulls overlap. This is due to the way the clustering technique works.
6. Use the convex hull information to find the centroids of these clusters. The  $n$  centroids represented as the  $(x,y)$  coordinates are the desired sample points.

While the above method is an approximate implementation, it has several advantages as follows:

1. It retains the space-filling properties;
2. The computational cost is very low compared to a true implementation that would require one to solve successive optimization problems for each set of samples;
3. The use of the clustering followed by choosing centroid points guarantees that the samples are 'inside' the domain and sufficiently away from each of the vertices; and,
4. Reproducibility.

#### 4.4 Polygon Design of Experiments (PDOE) Method

An alternate method to the LHS design was developed to account for a non-rectangular domain, given the reasons noted above. This method is referred to as the Polygon Design of Experiments (PDOE) method for brevity. The following sampling strategy was implemented, assuming that the compressor operating envelope is given and  $n$  total samples are desired:

1. Initialize empty sample set  $D$ .
2. Start with the compressor operating envelope represented as a polygon with  $k$  vertices.
3. Add these  $k$  vertices to  $D$ .
4. Sample the remaining  $(n-k)$  points using the non-rectangular sampling method described in the previous section.

The data representation methods are meant to be used for interpolation purposes. As such, adding the  $k$  initial vertices is the simplest and the logical starting point. The AHRI Standard 540 and four other alternate data representation methods found in the literature were analyzed with regards to the number of samples used in generating the performance map. The number of samples that were tried included [8, 10, 12, 14, 16]. Appropriate models were chosen for the different number of samples. For example, the AHRI Standard 540 model requires a minimum of 11 points and so it cannot be used with 8 and 10 samples. Furthermore, comprehensive data sets were available for three separate compressors. These datasets were analyzed separately from the normal (limited) data sets.

Results indicated that the LHS method provides a much better average prediction performance for a given number of samples, but it is quite possible that this performance may change for a different run of the LHS design. While the overall prediction using the LHS design is better, there are areas within the map where in the local errors are unacceptably high. In general, the AHRI Standard 540 model shows average errors below 1%. The maximum absolute errors, on the other hand, are relatively higher. Irrespective of the number of samples and the sampling method, the MAPE in predicted power is less than 5% for the AHRI Standard 540 and two other evaluated models.

## 5. CONCLUSIONS

There are several sources of uncertainty in the prediction of compressor performance using maps or models. The most important amongst them are the uncertainty due to measurement and the uncertainty due to regression during model development. The measurement uncertainty has been quantified in the literature. The regression uncertainty



was studied in the present work for the AHRI Standard 540 method. The worst case maximum absolute error in predicted mass flow rate across all data sets was 17% and that for power was 9%. For most compressors, the high errors occur in the region of the envelope with low suction and low discharge dew point temperatures. The average uncertainty in power prediction can be as high as 5% and that in mass flow rate prediction can be as high as 4%.

A study was conducted to evaluate the effect of sample size on the prediction capabilities for the various models. One of the challenges was the selection of samples from the operating envelope. The conventional LHS method was used as well as a new method (PDOE) from the literature for sampling on non-rectangular domains. For the case of mass flow rate, it was found that the LHS method yielded average errors lower than 2% for all the sample sizes. However, the maximum absolute errors in mass flow rate were higher when there were a lower ( $\leq 10$ ) number of samples. In general, both the LHS and PDOE methods yielded similar errors for all models for samples sizes of 12, 14 and 16. Thus, for mass flow rate, it is possible to build a model with 12 systematically selected test points. For power prediction, the average error for LHS and PDOE methods using AHRI Standard 540 and two other evaluated methods was lower than 2% for all sample sizes. In general, the errors were of similar magnitude for 12, 14 and 16 samples. For some cases with the LHS method, the errors were unusually high, due the random nature of the algorithm.

Based on the results of the analysis conducted, the following observations and recommendations are made to improve compressor data representation:

1. Reducing the measurement uncertainty is important. Particular attention must be paid during measurements involving low suction and low discharge dew point temperatures.
2. The regression uncertainty has an additive effect on the overall model prediction when the measurement uncertainty is factored into the overall model uncertainty. As such, it is possible to define a lower bound on the expected uncertainty in model prediction. Higher bounds may be possible depending on the availability of data.
3. In order to reduce the regression uncertainty, numerically stable and linearly regressed models should be selected, though this is not always possible for a physics-based power prediction model. Mass flow models can be adapted to linear regression.
4. There is potential for reducing the number of tests used to develop the performance map for a compressor. In general, for the models analyzed as a part of this work, a sample size of 10 or 12 is recommended. This requires additional verification.
5. The use of a systematic DOE method is recommended for selection of samples once an operating envelope is determined. It should be noted, however, that most DOE methods are designed to work with rectangular domains.

## NOMENCLATURE

T                      Temperature                      ( $^{\circ}\text{C}/^{\circ}\text{F}$ )

### Subscripts

c                      condenser  
e                      evaporator

### Abbreviations

|        |  |
|--------|--|
| A/C    | Air Conditioning   |
| AHRI   | Air Conditioning, Heating, and Refrigeration Institute                     |
| ASHRAE | American Society of Heating, Refrigerating, and Air-Conditioning Engineers |
| COV    | Coefficient of Variance  |
| DOE    | Design of Experiments  |
| HP     | Heat Pump  |
| LHS    | Latin Hypercube Sampling   |
| MAPE   | Maximum Absolute Percent Error   |
| PDOE   | Polygon Design of Experiments  |

## REFERENCES

ANSI/AHRI., 2015. Standard for Performance Rating of Positive Displacement Refrigerant Compressors and Compressor Units. Standard 540. Arlington, VA: AHRI.

Coleman, H. W., and Steele, W. G., 2009, Experimentation, Validation and Uncertainty Analysis for Engineers, Third Edition, John Wiley and Sons.

Draguljic D, Santner TJ, Dean AM. 2012, Noncollapsing Space-Filling Designs for Bounded Nonrectangular Regions, *Technometrics* 2012; 54(2):169–178.

Lekivetz, R. and Jones, B., 2014, Fast Flexible Space-Filling Designs for Nonrectangular Regions, *Research Article, Quality and Reliability Engineering International*, DOI:10.1002/qre.1640.

## ACKNOWLEDGEMENT

The authors would like to acknowledge AHRI and the members of the committee for Project 8013 for support of this analysis effort.